Life Sciences 239 (2019) 116879

Contents lists available at ScienceDirect

Life Sciences

journal homepage: www.elsevier.com/locate/lifescie

Icariin induces apoptosis of human lung adenocarcinoma cells by activating the mitochondrial apoptotic pathway

Xiaoli Wu[a,1], Wencui Kong[a,1], Xiaoyan Qi[b,1], Shuiliang Wang[c,d], Ying Chen[a], Zhongquan Zhao[a], Wenwu Wang[a], Xiandong Lin[e], Jinhuo Lai[f], Zongyang Yu[a,g,h,i,*], Guoxiang Lai[j,**]

[a] Department of Medical Oncology, 900 Hospital of the Joint Logistics Team Support Force, Fuzhou, Fujian Province, 350025, PR China
[b] Department of Oncology, Zibo Central Hospital, Zibo, Shandong Province, 255020, PR China
[c] Department of Urology, 900th Hospital of the Joint Logistics Team Support Force, Fujian Medical University, Fuzhou, Fujian Province, 350025, PR China
[d] Fujian Key Laboratory of Transplant Biology, Affiliated Dongfang Hospital, Xiamen University School of Medicine, Fuzhou, Fujian Province, 350025, PR China
[e] Laboratory of Radiation Oncology and Radiobiology, Fujian Cancer Hospital and Fujian Medical University Cancer Hospital, Fuzhou, Fujian Province, 350014, PR China
[f] Department of Oncology, Fujian Medical University Union Hospital, Fuzhou, Fujian Province, 350001, PR China
[g] Fujian Medical University Affiliated Dongfang Hospital, Fuzhou, Fujian Province, 350025, PR China
[h] Xiamen University School of Medicine, Xiamen, Fujian Province, 361102, PR China
[i] Fujian University of Traditional Chinese Medicine, Fuzhou, Fujian Province, 350122, PR China
[j] Department of Respiratory and Critical Care Medicine, 900 Hospital of the Joint Logistics Team Support Force, Fuzhou, Fujian Province, 350025, PR China

ARTICLE INFO

Keywords:
Icariin
Apoptosis
Mitochondrial pathway
Non-small cell lung cancer

ABSTRACT

Lung cancer is the largest cause of morbidity and mortality among tumor diseases. Traditional first-line chemotherapeutic drugs are frequently accompanied by serious side effects when used to treat tumors, thus, novel drugs with reduced toxic effects may improve a patients' quality of life. Icariin, an extract of herba epimedii, has been demonstrated to exhibit multiple antitumor effects with low toxicity. In the present study, cell cycle analysis, apoptosis assays, DAPI staining, CCK8 assays, xenograft tumor models, mitochondrial membrane potential analysis, western blotting and reverse transcription-quantitative PCR were performed to determine the molecular mechanism underlying icariin activity in the human lung adenocarcinoma cell lines, A549 and H1975. The results showed that icariin reduced proliferation of A549 and H1975 cells in a time- and dose-dependent manner in vitro to a greater degree than the control BEAS-2B cells, and this was associated with increased apoptosis, but not with cell cycle progression. In vivo experiments showed that icariin treatment significantly decreased proliferation of H1975 cells in a xenograft mouse model. Mechanistically, icariin activated the mitochondrial pathway by inhibiting the activation of the PI3K-Akt pathway-associated kinase, Akt, resulting in the activation of members of the caspase family of proteins, and thus inducing apoptosis of A549 cells. Taken together, the results revealed that icariin has anti-cancer properties in lung cancer in vitro and *in vivo* without any noticeable toxic effects on normal lung epithelial cells. Icariin in combination with conventional anti-cancer agents may be an effective therapeutic strategy for treatment of lung carcinoma.

1. Introduction

Lung cancer is a deadly cancer with the highest morbidity and mortality rates [1,2]. Worldwide, millions of people are diagnosed with lung cancer every year, and ~1,000,000 lung cancer patients suffer from cancer-associated deaths [3,4]. Non-small cell lung cancer (NSCLC) accounts for 80–85% of lung cancer cases. Patients with NSCLC frequently present with symptoms, such as hemoptysis and bloody sputum; however, the early symptoms are not always obvious [5–7]. A large proportion of patients are diagnosed with advanced stage lung cancer which has metastasized, meaning surgical resection is not an option [8–10]. In these cases, radiotherapy, chemotherapy, other targeted therapies and emerging immunotherapies are used. Chemical drug treatments are used before cisplatin, as a first line therapy for non-small cell lung cancer [11,12]. Due to the untargeted and nonselective nature of chemical drugs, they exhibit notable side effects on healthy

* Corresponding author. No.156, Xi'erhuan North Road, Fuzhou, Fujian Province, 350025, PR China.
** Corresponding author. No.156, Xi'erhuan North Road, Fuzhou, Fujian Province, 350025, PR China.
E-mail addresses: yuzongyang156@163.com (Z. Yu), laiguoxiang11@163.com (G. Lai).
[1] co-first authors. Xiaoli Wu, Wencui Kong and Xiaoyan Qi are equal to this work.

https://doi.org/10.1016/j.lfs.2019.116879
Received 16 July 2019; Received in revised form 7 September 2019; Accepted 15 September 2019
Available online 02 November 2019
0024-3205/

proliferating cells in the patients' body [13], thus resulting in hair loss [14,15] and diarrhea [16], significantly decreasing the patients' quality of life. Studies have shown that the vast majority of patients with NSCLC exhibit varying degrees of resistance to chemotherapeutic drugs [17,18]. Furthermore, certain chemotherapeutic drugs have been reported to induce distant metastasis of tumors [19–22]. Therefore, identifying and developing novel effective chemotherapeutic agents without or with reduced side effects will benefit patients with NSCLC.

In recent years, Chinese herbal medicines have attracted increasing attention in cancer research. Epimedium belongs to the *berberidaceae* genus, and is commonly used in a clinical setting [23]. Epimedium contains a variety of active ingredients, including flavonoids, volatile oils, polysaccharides and alkaloids. Recent studies suggest that epimedium strengthens the immunity of the body, improves cardiovascular blood flow, enhances the functioning of the reproductive system, promotes hematopoietic function, regulates the endocrine system, delays aging and exhibits anti-tumor activity [24–26]. Icariin is an effective monomer classified as a flavonoid [23–27]. Use of icariin for treating malignant tumors has been extensively studied. Icariin has been demonstrated to exhibit therapeutic effects in lung cancer [28], liver cancer [29] and esophageal cancer [30].

A previous study demonstrated that icariin treatment increased intracellular reactive oxygen species levels, reducing the mitochondrial membrane potential, activating caspase 3 and inducing apoptosis of liver cancer cells [31]. In breast cancer, icariin was found to induce G2/M phase arrest accompanied with down-regulation of Cyclin B, CDC2 and other genes [32]. In addition, a study on neovascularization measurements in fertilized eggs after 8 days, suggested that icariin reduced angiogenesis by acting on the chorioallantoic membrane of chicken embryos. By upregulating the activity of PERK and mediating the expression of GRP78 and CHOP, icariin may activate the endoplasmic reticulum stress pathway and induce the apoptosis of lung adenocarcinoma cells [28].

Although icariin exhibits desirable anti-tumor activity in a variety of different types of tumor, the structure and function of the molecule have not been fully elucidated. In our previous study, it was demonstrated that the apoptotic rate of A549 NSCLC cells treated with icariin was increased, similar to previous studies [28]. In addition to the changes in the expression levels of proteins involved in the endoplasmic reticulum stress pathway, the activity and expression levels of proteins involved in the mitochondrial apoptotic pathway were also significantly affected. When icariin was used to treat normal lung epithelial cells, no toxic effects were observed, suggesting that icariin may promote apoptosis of lung cancer cells by regulating the expression and activation of mitochondrial pathway-associated genes, without adverse effects on normal healthy cells. Therefore, understanding the molecular mechanism underlying icariin activity may support its use in a clinical setting.

2. Methods and materials

2.1. Cell lines and cell culture

A549, H1299 and H1975 human lung cancer cells and normal human lung epithelial BEAS-2B cells were obtained from Cell Bank of Shanghai Research Institute of Life Sciences and maintained in RPMI 1640 medium (Hyclone; GE Healthcare Life Sciences) supplemented with 10% FBS (Hyclone; GE Healthcare Life Sciences) and 1% penicillin-streptomycin (Beijing Solarbio Science & Technology Co., Ltd.) at 37 °C with 5% CO_2 in an incubator.

2.2. Preparation of the MK-2206 and icariin solutions

Akt inhibitor, MK-2206, and icariin powder (both from Sigma-Aldrich; Merck KGaA) were dissolved in DMSO (Beijing Solarbio Science & Technology Co., Ltd.). MK-2206 was diluted to a working concentration of 1 μM using culture medium and icariin was diluted to four different concentrations; 5, 10, 20 and 40 μM.

2.3. Cell proliferation assay

Cells were seeded in 96-well plates at 1×10^4 cells/well and treated with the various icariin concentrations for 24, 48 or 72 h. Subsequently, the medium was changed and 10% Cell Counting Kit-8 (CCK-8) reagent was added (cat. no. C0038; Beyotime Institute of Biotechnology), and cells were incubated for a further 2 h. Absorbance was measured at 450 nm using a microplate spectrophotometer (GE, USA). All assays were performed in triplicate.

2.4. DAPI staining

Cells were treated as described above, and the medium was replaced, cells were washed with PBS three times. Subsequently, cells were fixed with 4% paraformaldehyde for 30 min. Cells were permeabilized with 0.1% Triton X-100 for 10 min. After washing, DAPI stain (cat. no. C0065; Beijing Solarbio Science & Technology Co., Ltd.) was used to stain the cells for 5 min. Cells were observed under a fluorescence microscope (Olympus Corporation, Japan) and imaged.

2.5. Cell cycle and apoptosis analysis

Cells were plated in 6-well plates at a density of 8×10^5 cells/well and treated with the aforementioned concentrations of icariin. After 24–48 h, cells were harvested, resuspended in 70% pre-cooled ethanol in PBS and left at 4 °C overnight. Cells, were subsequently centrifuged at 700 × *g*, washed with 1 ml pre-cooled PBS, resuspended to a density of 1.0×10^6 cells/ml and stained with 20 μg/ml propidium iodide staining buffer (cat. no. C1052; Beyotime Institute of Biotechnology). Analysis was performed using flow cytometry (Beckman Coulter Gallios, USA) and all experiments were repeated three times.

2.6. Reverse transcription-quantitative (RT-q)PCR

Tumor cells were seeded in 6-well plates at a density of 8×10^5 cells/well and treated with icariin for 72 h. Total RNA was extracted using TRIzol reagent (Thermo Fisher Scientific, Inc.) according to manufacturer's protocol. The purity and concentration of total RNA were detected using ultraviolet spectrophotometer, and a 1.8–2.0 A260/A280 ratio was used as the threshold for good quality RNA. For reverse transcription, 1 μg total RNA was reversed transcribed to cDNA according to manufacturer's protocol (cat. no. AE341-02, TransGen Biotech, Beijing, China). The reverse transcription temperature protocol was 37 °C for 15 min and 85 °C for 5 s; after which DNA was held at 4 °C. qPCR primers were synthesized by Sangon Biotech Co., Ltd. qPCR was performed on an ABI7500 (Applied Bioscience; Thermo Fisher Scientific, Inc.). The amplification program used was as follows: 95 °C Pre-denature for 5 min; followed by 40 cycles of 95 °C denature for 30 s and 60 °C annealing for 15 s mRNA expression is presented as the fold change relative β-actin and was determined using the $2^{-\Delta\Delta Ct}$ method. Results were performed at least three times independently.

The sequences of all primers were as follows: caspase-3 forward, FAGAGGGGATCGTTGTAGAAGTC and reverse, ACAGTCCAGTTCTGTACCACG; caspase-9 forward, CTCAGACCAGAGATTCGCAAAC and reverse, GCATTTCCCCTCAAACTCTCAA; Akt forward, AGCGACGTGGCTATTGTGAAG and reverse, GCCATCATTCTTGAGGAGGAAGT; PI3K forward, AGAGCACTTGGTAATCGGAGG and reverse, CTTCCCCGGCAGTATGCTTC; Bax forward, CCCGAGAGGTCTTTTTCCGAG and reverse, CCAGCCCATGATGGTTCTGAT; Bad forward, CCCAGAGTTTGAGCCGAGTG; reverse, CCCATCCCTTCGTCGTCCT; and β-actin forward, CATGTACGTTGCTATCCAGGC and reverse CTCCTTAATGTCACGCACGAT.

2.7. Western blotting

Cells were lysed with RIPA lysis buffer (Beyotime Institute of Biotechnology) or NE-PER™ Nuclear and Cytoplasmic Extraction Reagent (cat. no. Thermo Fisher Scientific, Inc.). Protein concentration was detected using a bicinchoninic acid assay (Beyotime Institute of Biotechnology). Proteins were resolved on a 10% gel using SDS-PAGE and transferred onto PVDF membrane (EMD Millipore) using a semidry transfer system. After blocking with 5% skimmed milk at room temperature for 2 h, membranes were incubated with one of the following primary antibodies at 4 °C overnight: Rabbit anti-Bad (1:1,000; cat. no. ab32445), rabbit anti-Bad (phosphor-S112) (1:1,000; cat. no. ab129192), rabbit anti-human p-Bax (1:1,000; cat. no. ab111391), rabbit anti-human Bax (1:1,000; cat. no. ab53154), rabbit anti-human Akt (1:1,000; cat. no. ab185633), rabbit anti-human p-Akt (1:1,000; cat. no. ab192623), rabbit anti-human cleaved-caspase-3 (1:1,000; cat. no. ab2302), rabbit anti-cleaved-caspase-9 (1:1,000; cat. no. ab2324), mouse anti-human caspase-3 (1:1,000; cat. no. ab208161), mouse anti-human caspase-9 (1:1,000; cat. no. ab69541), mouse anti-cytochrome C antibody (1:1,000; cat. no. ab50050), rabbit anti-human COX IV2 (1:3,000; cat. no. ab16056), rabbit anti-human VDAC1 (1:3,500; cat. no. ab154856) and rabbit anti-human β-actin (1:5,000; cat. no. ab8227). Subsequently, the membranes were incubated with the corresponding horseradish peroxidase-conjugated secondary antibody (1:4,000; cat. nos. ab6721 and ab6789) for 3 h at room temperature and visualized using Millipore western blot kit (Merck KGaA). All antibodies were purchased from Abcam. The bands were obtained using Chemiluminescence Apparatus (General Electric Company) and quantified using Quantity One 4.6 (Bio-Rad Laboratories, Inc. USA). β-actin was used as the internal reference for total cell protein, and COX IV2 or VDAC1 were used as the internal references for total mitochondrial proteins. All experiments were repeated at least three times.

2.8. Isolation of mitochondrial proteins and cytoplasmic proteins

Phenylmethylsulfonyl fluoride (PMSF; cat. no. P8340; Beijing Solarbio Science & Technology Co., Ltd.) crystals were added to 1.5 ml PMSF solvent to a final concentration of 100 mM PMSF. PMSF solution was further diluted to a working concentration of 1 μM. Cells were washed with PBS, digested with trypsin, centrifuged at 600 × *g* at 4 °C for 5 min, resuspended with pre-cooled PBS and centrifuged again for 5 min at 4 °C. The supernatant was discarded, and the cells were treated with 1–2.5 ml NE-PER™ Nuclear and Cytoplasmic Extraction Reagents for 10–15 min on ice. The cell suspension was transferred to a glass homogenizer and homogenized with 10–30 passes. Subsequently, cell homogenate was centrifuged at 600 × *g* at 4 °C for 10 min. The supernatant was collected and centrifuged at 11,000 × *g* at 4 °C for 10 min, of which, the supernatant contained the cytoplasmic proteins and the precipitate contained the isolated cell mitochondria. Finally, 150–200 μl mitochondrial lysis buffer (cat. no. C3601, Beyotime Biotechnology, Beijing, China) was added to obtain protein samples for western blotting.

2.9. Mitochondrial membrane potential assay

JC-1 (50 μl; 200x; cat. no. C2006; Beyotime Biotechnology, Beijing, China) was added to 8 ml of ultrapure water and vigorously vortexed. From this, 2 ml JC-1 staining buffer (5x), was mixed with ddH_2O to obtain the working solution. Cells were trypsinized and centrifuged at 200 × *g* for 3 min. A total of 6×10^5 cells were collected in 0.5 ml cell culture medium, and 0.5 ml of JC-1 staining solution was added. The cells were inverted several times to ensure equal mixing of the staining buffer, after which they were incubated at 37 °C for 20 min. During the incubation, 1x JC-1 staining buffer was prepared on ice according to the manufacturer's protocol. After incubation, the cells were pelleted by centrifugation at 600 × *g* for 4 min at 4 °C. The supernatant was discarded, the cells were washed twice with 1x JC-1 staining buffer, and then resuspended in 1x JC-1 staining buffer. The cells were analyzed using a flow cytometer. The excitation wavelength was set to 490 nm and the emission wavelength was set to 530 nm for detection of the JC-1 monomer. For detection of the JC-1 polymer, the excitation wavelength was set to 525 nm, and the emission wavelength was set to 590 nm.

2.10. Animal experiments

All animal experiments performed in the present study were approved by the Animal Care Committee of the 900 Hospital of the Joint Logistics Team Support Force (Fuzhou, China). For the xenograft tumor model, 1×10^6 H1975 cells in 0.2 ml PBS were subcutaneously inoculated into the back of 8-week-old nude mice (n = 18), which were randomly divided into three groups, 6 nude mice per a group. One group of mice were treated with 3 mg/kg icariin every 3 days and another group of mice were treated with 10 mg/kg icariin every 3 days. The remaining group of mice was used as the control, which received the same volume of PBS. Nude mice were kept at a appropriate temperature (25 °C ± 1 °C) and a relative humidity of 50 ± 10% under a 12-h light–dark cycle. The tumor diameter was measured every 7 days with digital calipers and the volume of the excised tumor was measured on day 42 after the animals were sacrificed by cervical dislocation.

2.11. Statistical analysis

Data analysis was performed using SPSS version 21.0 (IBM Corp.). All experiments were repeated at least three times independently. Data are presented as the mean ± standard deviation. Differences between two groups were determined using a Student's t-test. Differences between ≥3 groups were determined using a one-way ANOVA with a post hoc Dunnett's test. $P < 0.05$ was considered to indicate a statistically significant difference.

3. Results

3.1. Icariin reduces proliferation of A549, H1299 and H1975 cells

To determine the effect of icariin on NSCLC cells, A549, H1299 and H1975 cells were treated with various concentrations of icariin and a CCK8 assay was used to measure proliferation. Icariin significantly reduced proliferation of A549, H1299 and H1975 NSCLC cells in time- and dose-dependence manner, compared with the respective control group ($P < 0.05$; Fig. 1A–C). Furthermore, based on the xenograft mouse model, icariin significantly reduced the proliferation of H1975 lung adenocarcinoma cells in a dose-dependent manner *in vivo* (Fig. 1D–F; $P < 0.05$).

3.2. Icariin induces the apoptosis of A549 cells independent of cell cycle regulation

To determine the mechanism by which icariin exerted its effects on NSCLC cells, A549 cells were treated with different concentrations of icariin. Flow cytometry was used to detect the proportion of cells in each stage of the cell cycle and the apoptotic rate. Icariin significantly increased the apoptotic rate of A549 cells in a dose-dependent manner compared with the control group ($P < 0.05$; Fig. 2). However, there was no significant change observed in the proportion of cells in each stage of the cell cycle in the A549 cells ($P > 0.05$). After observing and counting the number of adherent cells under the microscope, it was shown that treatment with icariin for 48 h reduced the number of adherent cells in a dose-dependent manner compared with the control ($P < 0.05$). Furthermore, nucleic heterogeneity of A549 cells was increased after icariin treatment as shown by DAPI staining, with chromatin concentration and fragmentation observed, similar to what was

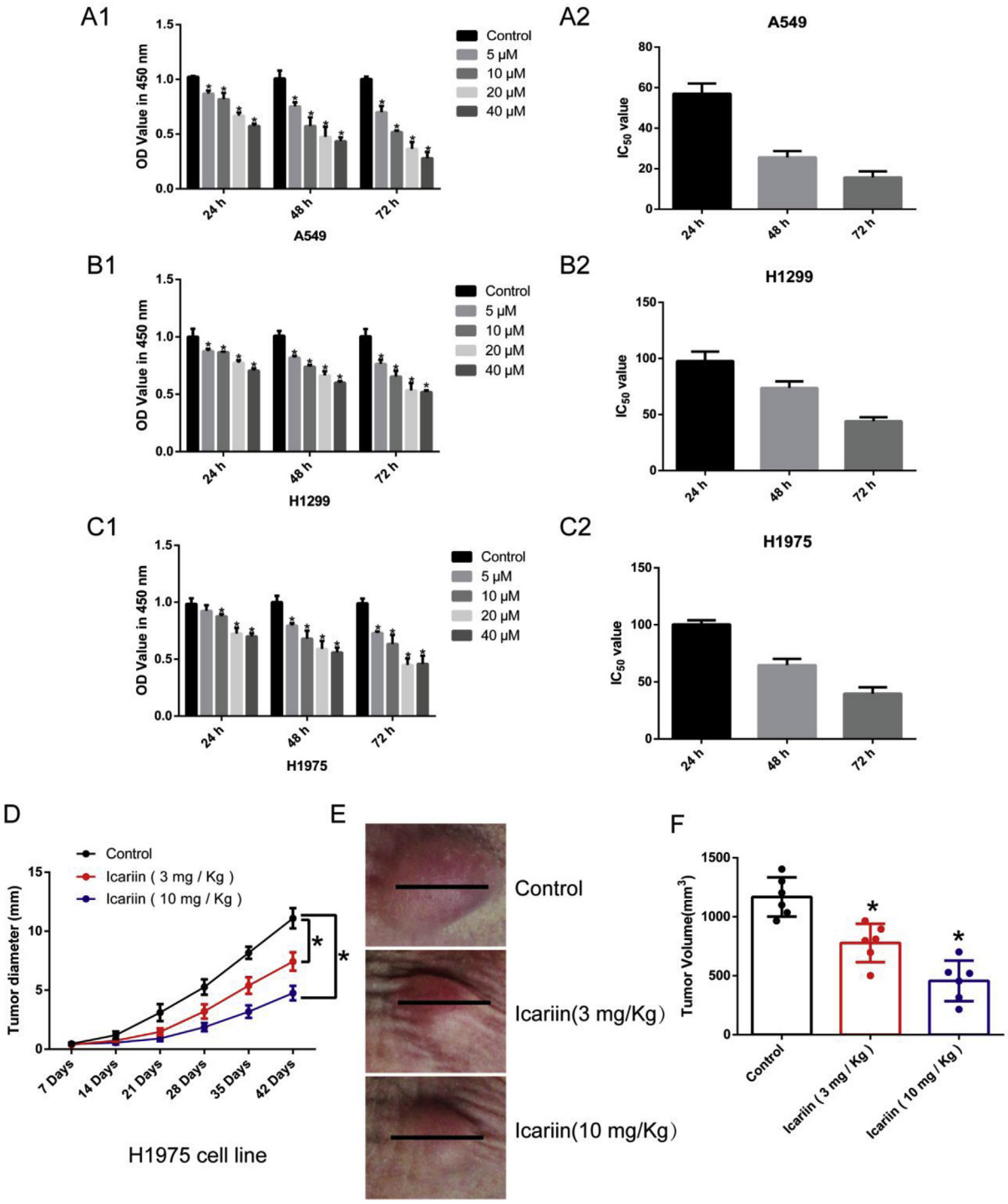

Fig. 1. Effect of icariin on proliferation of A549, H1299 and H1975 non-small cell lung cancer cells. Cell Counting Kit-8 assays showed that icariin decreased proliferation of (A) 1) A549 cells, (B) 1) H1299 cells and (C) 1) H1975 cells in a dose-dependent manner. Effect of IC_{50} values of icariin on (A) 2) A549 cells, (B) 2) H1299 cells and (C) 2) H1975 cells treated for 24, 48 or 72 h. (D) Tumor growth curve in the mice treated with 3 mg/kg, 10 mg/kg icariin or without icariin. The diameter of the tumor nodule was measured every 7 days after injection of cells and intragastric administration of icariin solution. (E) Representative images of the tumor nodule size measured in euthanized mice 42 days after injection of cells. Scale bar, 1 cm. (F) Quantitative analysis of tumor nodule volume 42 days after injection of cells. *P < 0.05 vs. control group. OD, optical density.

observed in the H1975 cells.

3.3. Icariin has no observable toxic effects on the normal lung epithelial BEAS-2B cells

To verify whether icariin induced apoptosis in lung cancer cells and determine any toxic effects on normal cells, lung epithelial BEAS-2B cells were cultured as described above and treated with 5, 10, 20 and 40 μM icariin for 24, 48 and 72 h. Untreated cells were used as the control group. Subsequently, a CCK8 assay, and apoptotic and cell cycle distribution analysis were performed. The above concentrations of icariin had no significant effect on the proliferation of BEAS-2B cells compared with the control (Fig. 3). Although the 40 μM icariin treatment decreased the proliferation and increased the apoptotic rate of

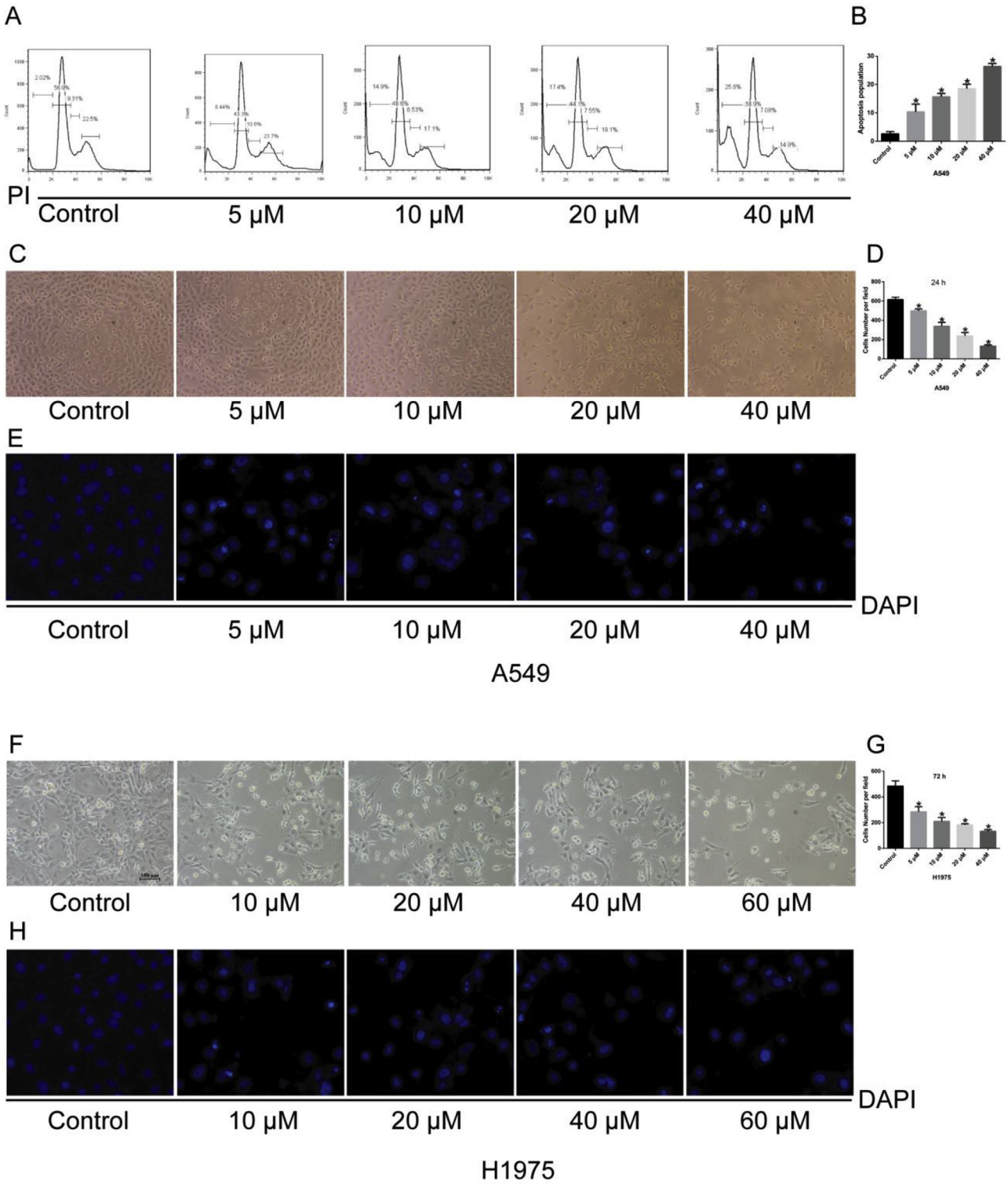

Fig. 2. Effects of icariin on apoptosis and proportion on cell cycle distribution of A549 cells. (A) Representative images of icariin induced apoptosis in A549 non-small cell lung cancer cells. (B) Quantitative analysis of icariin-induced apoptosis in A549 cells. (C) Representative images of adherent A549 cells treated with various concentrations of icariin. Magnification, x200. (D) Quantitative analysis of adherent A549 cells treated with different concentrations of icariin. (E) A549 cells were treated with different concentrations of icariin and the nuclear morphology was observed using DAPI staining. Magnification, x400. (F) Representative images of H1975 ells treated with different concentrations of icariin. Magnification, x200. (G) Quantitative analysis of the number of cells in five fields of view after treatment of H1975 cells with different concentrations of icariin. (H) H1975 cells were treated with different concentrations of icariin and the nuclear morphology was observed using DAPI staining. Magnification, x400. *P $<$ 0.05 vs. control group. PI, propidium iodide.

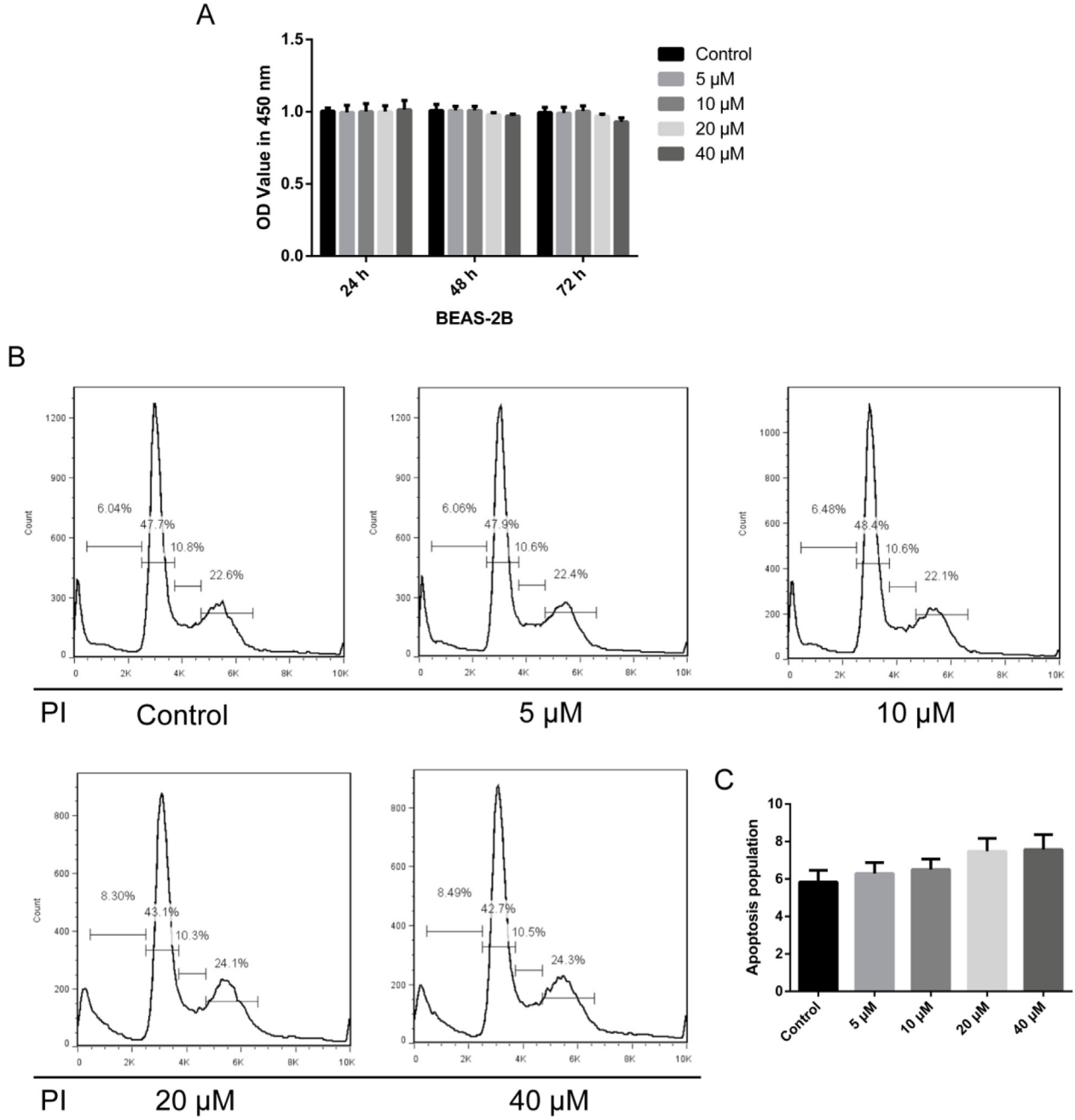

Fig. 3. Effect of icariin on lung epithelial BEAS-2B cells. (A) Different concentrations of icariin had no effect on the proliferation of BEAS-2B cells. (B) Flow cytometry analysis of apoptosis treated with various concentrations of icariin had no significant effect on apoptosis on BEAS-2B cells. (C) Quantitative analysis of flow cytometry data showed that icariin did not affect apoptosis of human normal lung epithelium BEAS-2B cells. PI, propidium iodide.

BEAS-2B cells compared with the control group, these differences were not statistically significant difference ($P > 0.05$). In addition, 40 μM icariin treatment did not significantly effect cell cycle distribution of BEAS-2B cells ($P > 0.05$).

3.4. Icariin treatment increases the mitochondrial membrane potential in A549 cells

To examine the molecular mechanism by which icariin decreased the proliferation of A549 cells, cells were treated with 40 μM icariin and mitochondrial membrane potential was measured using flow cytometry. Compared with the control group, icariin significantly decreased the mitochondrial membrane potential in a dose-dependent manner (Fig. 4; $P < 0.05$). In H1975 cells treated with icariin, the mitochondrial membrane potential of these cells decreased significantly. Additionally, icariin treatment significantly increased the activation of caspase-9 and caspase-3, but had no significant effect on the expression of total caspase-9 and caspase-3. Furthermore, icariin treatment significantly inhibited the phosphorylation of Akt and downregulated the phosphorylation of Bad and Bax.

3.5. Icariin treatment increases the levels of Bad and Bax in the mitochondria of A549 cells

In A549 cells treated with 40 μM icariin, the expression and activation of the mitochondrial apoptosis pathway-associated proteins, Bad and Bax, and changes to sub-localization were determined. There was no significant difference in the total expression of Bad and Bax

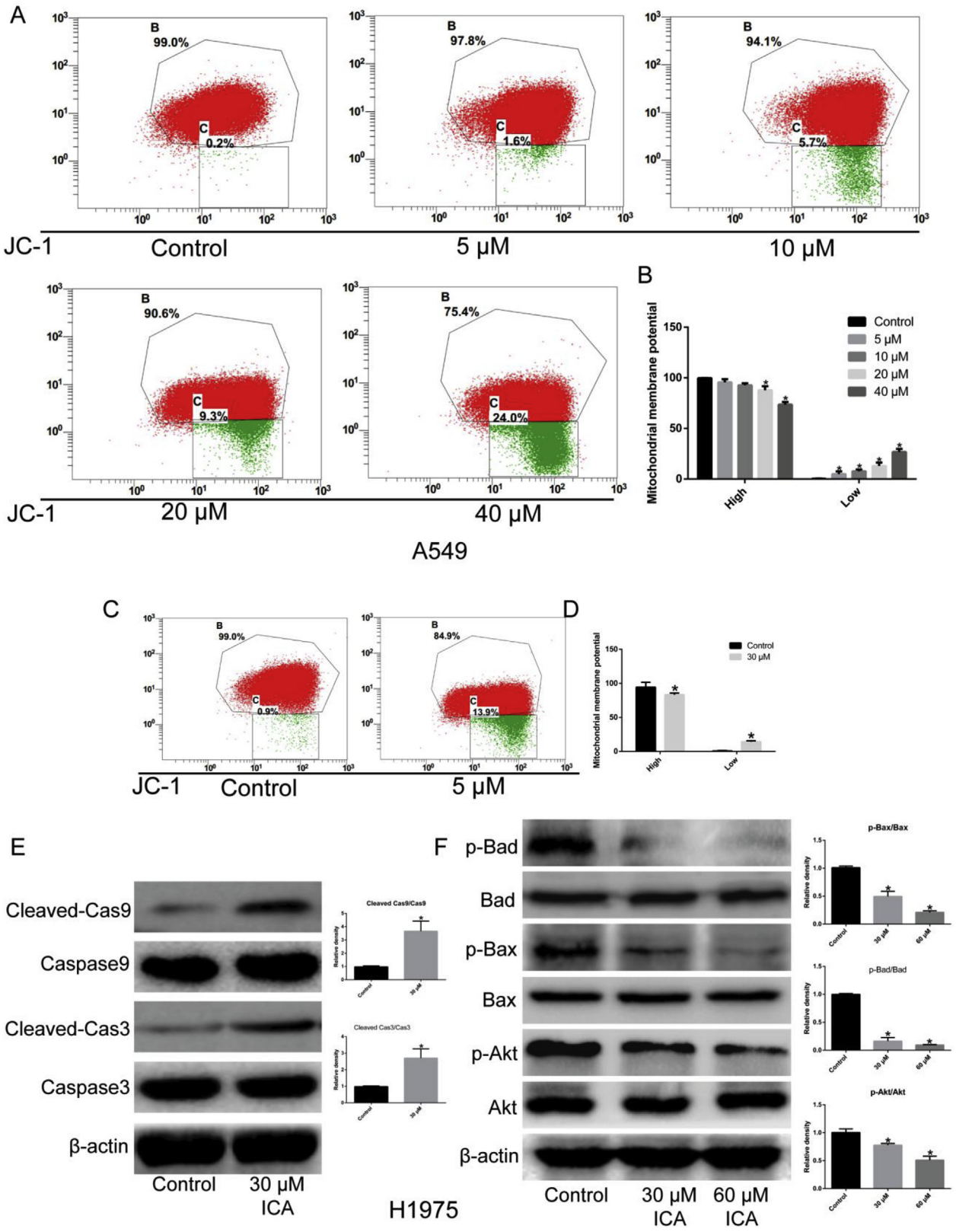

Fig. 4. Effect of icariin treatment on mitochondrial membrane potential in A549 cells. (A and B) Effect of different concentrations of icariin on mitochondrial membrane potential in A549 cells. (C and D) Effect of 30 μM icariin on the mitochondrial membrane potential in H1975 cells. (E) Icariin treatment significantly increased the activation of caspase-9 and caspase-3 in H1975 cells as shown by an increase in the cleavage of these caspases. (F) Icariin treatment significantly decreased the phosphorylation of Bad, Bax and Akt in dose-dependent manner. *P < 0.05 vs. control. ICA, icariin.

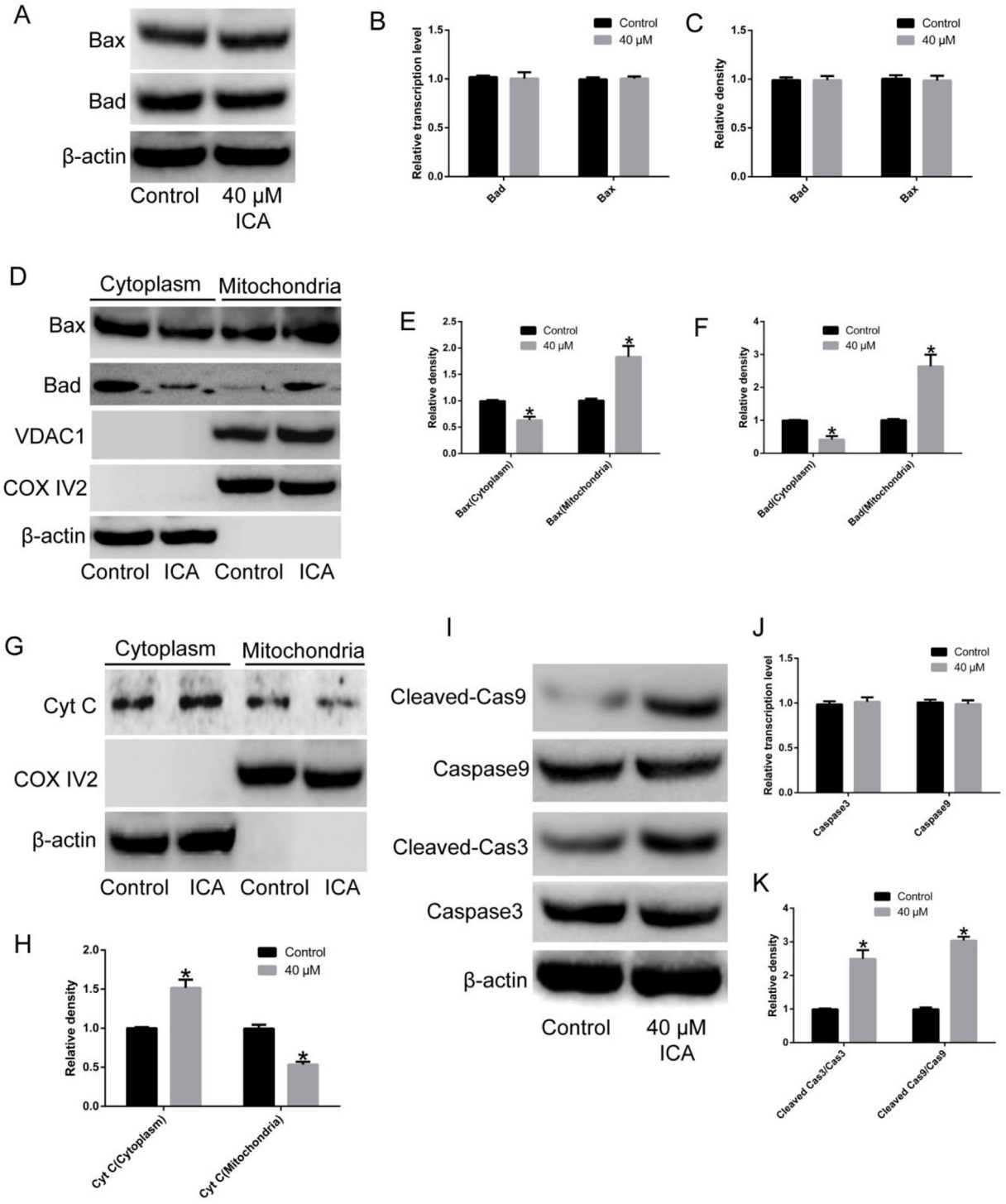

Fig. 5. Effect of icariin treatment on the levels of Bad and Bax in the mitochondria of A549 cells. (A) Representative blots showing the expression of mitochondrial pathway-associated proteins, Bad and Bax, detected using western blotting in A549 cells treated with 40 μM icariin. (B) mRNA expression levels of Bad and Bax in A549 cells. (C) Densitometry analysis of protein expression levels of Bad and Bax in A549 cells. (D) Representative blots demonstrating the distribution of Bad and Bax in the cytoplasm and mitochondria of A549 cells treated with 40 μM. Densitometry analysis of protein expression levels of (E) Bax and (F) in the cytoplasm and mitochondria of A549 cells. (G) Representative blots showing Cytochrome C distribution in the cytoplasm and mitochondria of A549 cells treated with 40 μM icariin. (H) Densitometry analysis of protein expression levels of Cytochrome C in the cytoplasm and mitochondria. (I) Representative blots showing the expressions of caspase-9 and caspase-3 and their cleaved variants in A549 cells treated with 40 μM icariin. (J) mRNA expression levels of caspase-9 and caspase-3 in cells treated with 40 μM icariin. (K) Densitometry analysis of activation of caspase-9 and caspase-3 based on cleavage of these caspases. *P < 0.05 vs. control. ICA, icariin.

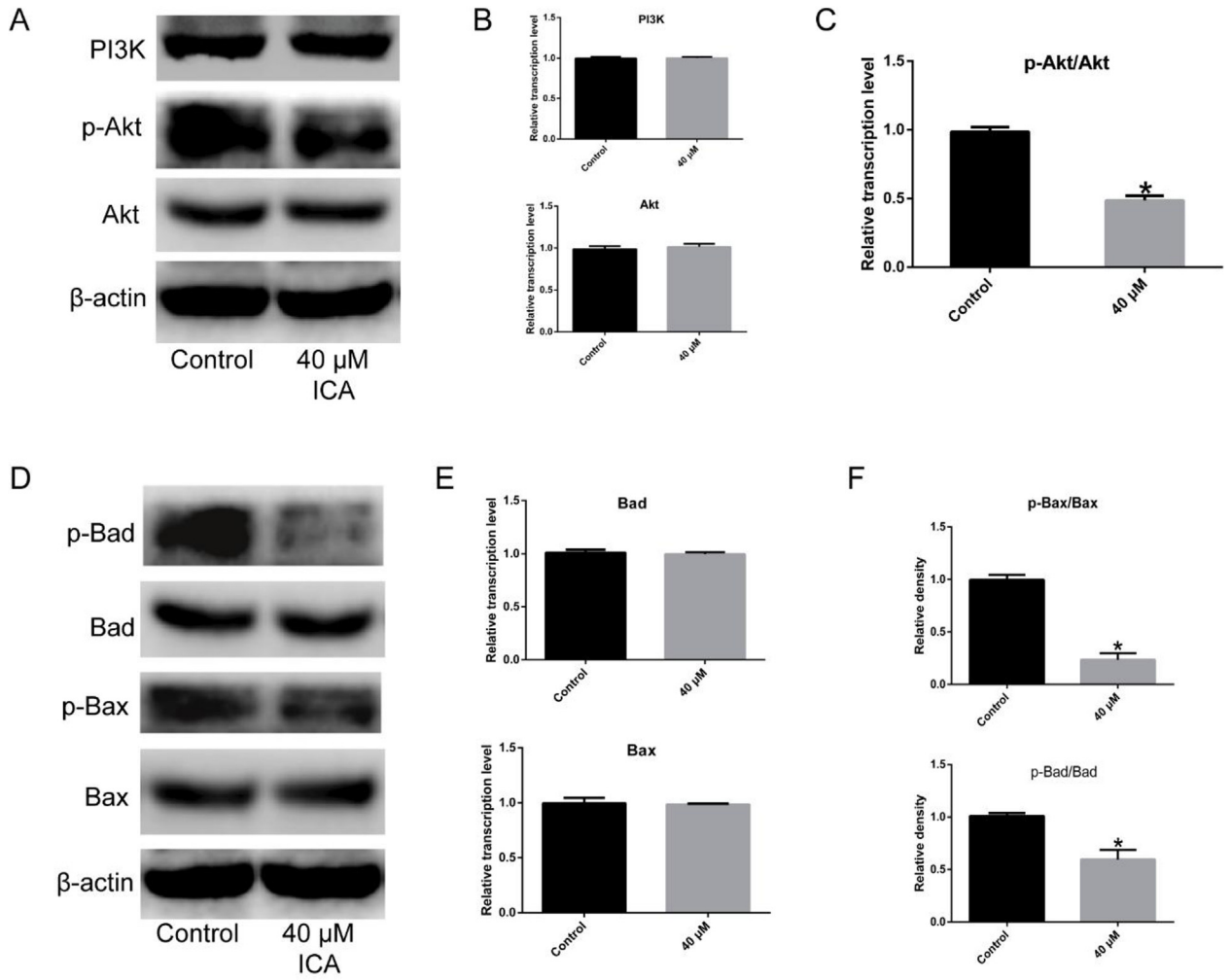

Fig. 6. Effect of icariin treatment on activation of the PI3K-Akt pathway and phosphorylation of Bad and Bax in A549 cells. (A) Representative blots showing the expression and activation levels of PI3K-Akt pathway-associated proteins PI3K and Akt, in A549 cells treated with 40 μM icariin. (B) mRNA expression levels of PI3K and Akt in A549 cells. (C) Quantitative analysis of the p-AKT/AKT ratio in A549 cells treated with 40 μM icariin. (D) Representative blots showing the phosphorylation levels of Bad and Bax. (E) mRNA expression levels of Bad and Bax in A549 cells treated with 40 μM icariin. (F) Quantitative analysis of the ratio of p-Bax/Bax and p-Bad/Bad in A549 cells treated with 40 μM icariin. *P < 0.05 vs. the control. ICA, icariin.

compared to the control (Fig. 5; P > 0.05), although the levels of both Bad and Bax were significantly increased in the mitochondria (Fig. 5; P < 0.05). Furthermore, the levels of cytochrome C in mitochondria were significantly decreased compared with the control (Fig. 5; P < 0.05) and activation of caspase-9 and caspase-3 were significantly increased (P < 0.05).

3.6. Icariin treatment decreases activation of the PI3K-Akt pathway and reduces phosphorylation of Bad and Bax

Following treatment of A549 cells with 40 μM icariin, the expression levels and activation of proteins involved in the PI3K-Akt pathway, and the phosphorylation levels of Bad and Bax were determined. Compared with the control, the expression levels of total PI3K and Akt did not change significantly (Fig. 6; P > 0.05); however, the activation levels of Akt was significantly decreased (P < 0.05). Furthermore, there were no significant changes in the total expression levels of Bad and Bax compared with the control (P > 0.05), similar to the above results, and the phosphorylation levels were significantly decreased (P < 0.05).

3.7. Icariin combined with the Akt inhibitor MK-2206, significantly decreases the proliferation of A549 cells

The above results preliminarily suggested that icariin regulated the activation of the mitochondrial pathway and induced apoptosis of A540 lung cancer cells by inhibiting the phosphorylation of Akt. When cells were co-treated with 1 μM MK-2206 and 20 μM icariin for 24 h, the proliferation of A549 cells was decreased significantly compared with either icariin or MK-2206 alone (Fig. 7A; P < 0.05). Apoptotic analysis using flow cytometry also showed that proportion of apoptotic cells was significantly increased in cells co-treated with icariin and MK-2206 compared either treatment alone (Fig. 7B and C; P < 0.05). Therefore, it was concluded that icariin (Fig. 7D) may activate the mitochondrial apoptosis pathway by inhibiting the PI3K/Akt signaling pathway, resulting in damage to the mitochondria, followed by the release of cytochrome C from the mitochondria to cytoplasm and activation of the downstream of apoptotic pathway (Fig. 7E).

4. Discussion

The incidence and mortality of lung cancer is highest among all types of malignant tumors [4,33]. Although many small-molecule drugs and cellular immunotherapy have been used in clinical or pre-clinical

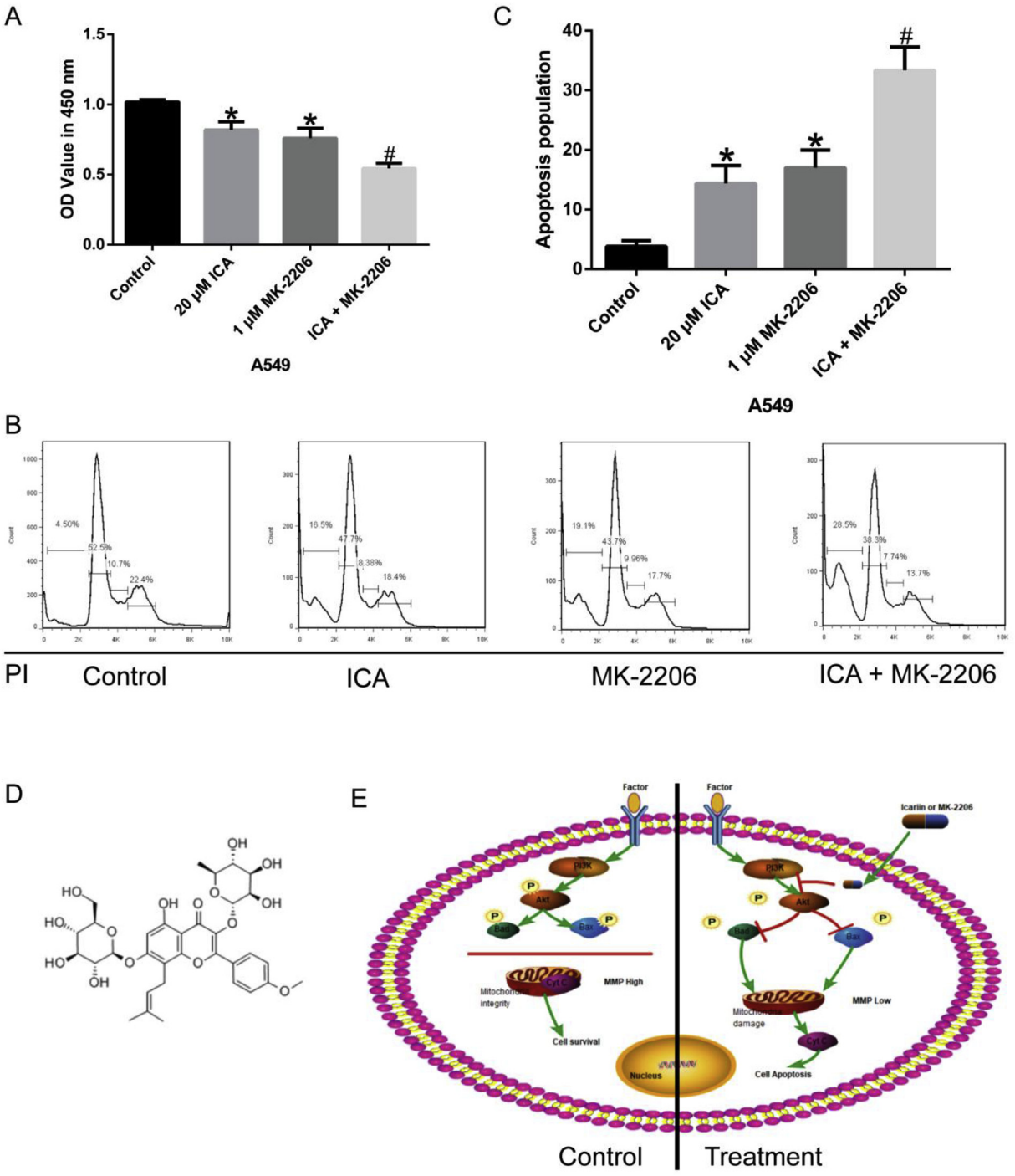

Fig. 7. Effect of combined treatment with icariin and the Akt inhibitor MK-2206 on proliferation of A549 cells. (A) Proliferation of A549 cells was significantly decreased by combined treatment with icariin and MK2206 compared with either treatment alone. (B) Representative flow cytometry data showing the proportion of apoptotic cells. Cells treated with icariin and MK-2206 alone or in combination increased apoptosis of A549 cells. (C) Quantitative analysis of apoptosis in A549 cells. (D) Structure of icariin. (E) Proposed schematic by which icariin increased apoptosis of lung adenocarcinoma cells. Icariin induced apoptosis of lung adenocarcinoma cells by regulating the PI3K-Akt pathway. *P $<$ 0.05 vs. control. $^{\#}$P $<$ 0.05 vs. icariin or MK-2206 treatment alone. OD, optical density; ICA, icariin; PI, propidium iodide.

trials [34,35], for the vast majority of patients, surgery combined with radiotherapy and chemotherapy is the first line of treatment [9,36]. However, chemoradiotherapy causes notable damage to patients' normal tissues, and the side effects significantly reduce the patients quality of life [13]. Therefore, novel compounds with reduced toxicity are required for treatment of lung cancer.

In recent years, Chinese herbal extracts have attracted increasing attention due to their regulatory effects on various biological processes and low toxicity [37]. Icariin, a flavonoid [29,30], has a variety of anti-tumor activities [29,30,38,39]. It has been reported that icariin causes an imbalance of the endoplasmic reticulum stress pathway in lung adenocarcinoma cells, resulting in the cells apoptosing [28]. In the present study, similar inhibitory effects of icariin on the proliferation of lung cancer cells both in vitro and *in vivo* were observed, which were primarily associated with increased apoptosis of lung cancer cells, without affecting cell cycle distribution. Additionally, icariin did not

exhibit any toxic effects on normal lung epithelial BEAS-2B cells.

Apoptosis is a form programmed cell death with complex and diverse underlying mechanisms. When cells are stimulated by physical stimuli, drugs or radiation, they transfer these signals into intracellular environment through receptors [40,41]. Imbalances in the endoplasmic reticulum stress pathway is one of the causes of apoptosis [42]. Additionally, reduction of the mitochondrial membrane potential leads to the release of mitochondrial contents, which further activate caspases, which are known as the executor of apoptosis, and finally induce apoptosis [43,44]. The results of the present study suggested that icariin treatment significantly reduced the mitochondrial membrane potential, and cytochrome C was released from the mitochondria into the cytoplasm. The release of cytochrome C is generally considered a marker of decreased mitochondrial membrane potential and the beginning of apoptosis [45,46]. Furthermore, Bad and Bax were enriched in the mitochondria following icariin treatment. Bad and Bax combine with pro-survival genes, including Bcl-xl, forming a complex which eliminate the protective effects of Bcl-xl, resulting in a decrease of the mitochondrial membrane potential and the initiation of apoptosis [47–49]. Similar to a previous study, activation of caspase-9 and caspase-3 was observed. Morphologically, typical apoptotic changes in nuclei of lung adenocarcinoma cells were observed by DAPI staining after icariin treatment.

Although our study preliminarily suggested that icariin may affect the mitochondrial membrane potential by regulating the subcellular localization of Bad and Bax in lung cancer cells, the molecular mechanism of activity was not elucidated. The activation of the PI3K-Akt pathway serves an important role in the proliferation, survival and drug resistance of lung cancer cells [50,51]. Studies have shown that icariin regulated the PI3K-Akt pathway [38,39,52]. In the present study, the results showed that icariin did not significantly alter the expression of PI3K and Akt at the transcriptional or translational levels in treated lung cancer cells, but phosphorylation of Akt was significantly reduced. Akt phosphorylates the mitochondrial apoptosis pathway-associated proteins Bad and Bax, thus changing their subcellular localization. The phosphorylated Bad and Bax tend to stay in the cytoplasm [53,54]. Similarly, the results of the present study also demonstrated that icariin treatment regulated the phosphorylation levels of Bad and Bax. Therefore, it is hypothesized that icariin attenuated the activation of Akt by targeting PI3K, preventing the phosphorylation of Bad and Bax. Additionally, combined treatment of cells with MK-2206 and icariin enhanced the inhibitory effects on cell proliferation and significantly and increased the proportion of apoptosis cell, suggesting that icariin in combination with other therapeutic compounds may improve the management of lung cancer in the future.

In conclusion, icariin reduced the phosphorylation levels of Akt by inhibiting PI3K. Bad and Bax phosphorylation was decreased and their cytoplasmic presence increased as a result. The mitochondrial membrane potential was decreased in cells treated with icariin which resulted in apoptosis. Icariin did not exhibit any significant toxic effects on normal lung epithelial BEAS-2B cells. Therefore, icariin may be used a potential drug or adjuvant for treating lung cancer.

Author contributions

Zongyang Yu and Guoxiang Lai designed the study. Xiaoli Wu, Wencui Kong and Xiaoyan Qi wrote this manuscript. Xiaoli Wu, Wencui Kong and Xiaoyan Qi, Shuiliang Wang, Ying Chen, Zhongquan Zhao, Wenwu Wang, Xiandong Lin and Jinhuo Lai performed the research, analyzed data. All authors read and approved the final manuscript.

Funding

This work was supported by Joint Funds for the Innovation of Science and Technology from Fujian Province (No.2017Y9127).

Declaration of competing interest

The authors have no conflicts of interest to disclose.

Acknowledgments

Not applicable.

References

[1] Y. Mao, D. Yang, J. He, M.J. Krasna, Epidemiology of lung cancer, Surg. Oncol. Clin. N. Am. 25 (3) (2016) 439–445, https://doi.org/10.1016/j.soc.2016.02.001 Epub 2016/06/05. PubMed PMID: 27261907.

[2] P. Nanavaty, M.S. Alvarez, W.M. Alberts, Lung cancer screening: advantages, controversies, and applications. Cancer control, J. Moffitt Canc. Cent. 21 (1) (2014) 9–14, https://doi.org/10.1177/107327481402100102 Epub 2013/12/21. PubMed PMID: 24357736.

[3] R.L. Siegel, K.D. Miller, A. Jemal, Cancer statistics, 2017, CA A Cancer J. Clin. 67 (1) (2017) 7–30, https://doi.org/10.3322/caac.21387 Epub 2017/01/06. PubMed PMID: 28055103.

[4] W. Chen, R. Zheng, P.D. Baade, S. Zhang, H. Zeng, F. Bray, et al., Cancer statistics in China, 2015, CA A Cancer J. Clin. 66 (2) (2016) 115–132, https://doi.org/10.3322/caac.21338 Epub 2016/01/26. PubMed PMID: 26808342.

[5] J. Yue, Q. Shi, T. Xu, M. Jeter, T.Y. Chen, R. Komaki, et al., Patient-reported lung symptoms as an early signal of impending radiation pneumonitis in patients with non-small cell lung cancer treated with chemoradiation: an observational study, Qual. Life Res. : Int. J. Qual. Life Aspects Treat. Care Rehabil. 27 (6) (2018) 1563–1570, https://doi.org/10.1007/s11136-018-1834-3 Epub 2018/03/20. PubMed PMID: 29549533; PubMed Central PMCID: PMCPMC5953814.

[6] T. Ando, H. Kage, M. Saito, Y. Amano, Y. Goto, J. Nakajima, et al., Early stage non-small cell lung cancer patients need brain imaging regardless of symptoms, Int. J. Clin. Oncol. 23 (4) (2018) 641–646, https://doi.org/10.1007/s10147-018-1254-y Epub 2018/02/28. PubMed PMID: 29484515.

[7] C.B. Falkson, Yu E. Vella ET, M. El-Mallah, R. Mackenzie, P.M. Ellis, et al., Radiotherapy with curative intent in patients with early-stage, medically inoperable, non-small-cell lung cancer: a systematic review, Clin. Lung Cancer 18 (2) (2017) 105–121.e5, https://doi.org/10.1016/j.cllc.2016.10.008 Epub 2016/12/03. PubMed PMID: 27908621.

[8] D. Ulahannan, J. Khalifa, C. Faivre-Finn, S.M. Lee, Emerging treatment paradigms for brain metastasis in non-small-cell lung cancer: an overview of the current landscape and challenges ahead, Ann. Oncol. : Off. J. Eur. Soc. Med. Oncol. 28 (12) (2017) 2923–2931, https://doi.org/10.1093/annonc/mdx481 Epub 2017/10/19. PubMed PMID: 29045549.

[9] P.S. Tan, M. Bilger, G. de Lima Lopes, S. Acharyya, B. Haaland, Meta-analysis of first-line therapies with maintenance regimens for advanced non-small-cell lung cancer (NSCLC) in molecularly and clinically selected populations, Canc. Med. 6 (8) (2017) 1847–1860, https://doi.org/10.1002/cam4.1101 Epub 2017/07/05. PubMed PMID: 28675660; PubMed Central PMCID: PMCPMC5548880.

[10] M. Lanuti, Surgical management of oligometastatic non-small cell lung cancer, Thorac. Surg. Clin. 26 (3) (2016) 287–294, https://doi.org/10.1016/j.thorsurg.2016.04.002 Epub 2016/07/19. PubMed PMID: 27427523.

[11] C. Zhao, H. Sun, Y. Yang, X. Dai, [Pemetrexed combined DDP in the treatment of advanced non-small cell lung cancer: a case report and literature review], Zhongguo fei ai za zhi = Chin. J. Lung Canc. 13 (7) (2010) 755–758, https://doi.org/10.3779/j.issn.1009-3419.2010.07.18 Epub 2010/08/03. PubMed PMID: 20673495; PubMed Central PMCID: PMCPMC6000374.

[12] M. Liao, Non-surgical therapy for patients with advanced non-small cell lung cancer, Respirology 3 (3) (1998) 151–157 Epub 1998/10/10. PubMed PMID: 9767613.

[13] X. Liu, L. Ma, K. Yang, J. Tian, [Vinorelbine plus oxaliplatin versus vinorelbine plus cisplatin for advanced non-small cell lung cancer: a systematic review], Zhongguo fei ai za zhi = Chin. J. Lung Canc. 13 (2) (2010) 112–117, https://doi.org/10.3779/j.issn.1009-3419.2010.02.06 Epub 2010/08/03. PubMed PMID: 20673502; PubMed Central PMCID: PMCPMC6000518.

[14] X. Wang, Y. Chen, Y. Tao, Y. Gao, D. Yu, H. Wu, A666-conjugated nanoparticles target prestin of outer hair cells preventing cisplatin-induced hearing loss, Int. J. Nanomed. 13 (2018) 7517–7531, https://doi.org/10.2147/ijn.s170130 Epub 2018/12/12. PubMed PMID: 30532536; PubMed Central PMCID: PMCPMC6241721.

[15] K. Tani, K. Tabuchi, A. Hara, Hair cell loss induced by sphingosine and a sphingosine kinase inhibitor in the rat cochlea, Neurotox. Res. 29 (1) (2016) 35–46, https://doi.org/10.1007/s12640-015-9563-7 Epub 2015/10/17. PubMed PMID: 26472207.

[16] R.Y. Tsang, T. Al-Fayea, H.J. Au, Cisplatin overdose: toxicities and management, Drug Saf. 32 (12) (2009) 1109–1122, https://doi.org/10.2165/11316640-000000000-00000 Epub 2009/11/18. PubMed PMID: 19916578.

[17] L. He, L. Luo, H. Zhu, H. Yang, Y. Zhang, H. Wu, et al., FEN1 promotes tumor progression and confers cisplatin resistance in non-small-cell lung cancer, Molecular oncology 11 (6) (2017) 640–654, https://doi.org/10.1002/1878-0261.12058 Epub 2017/04/04. PubMed PMID: 28371273; PubMed Central PMCID: PMCPMC5467497.

[18] D.A. Fennell, Y. Summers, J. Cadranel, T. Benepal, D.C. Christoph, R. Lal, et al., Cisplatin in the modern era: the backbone of first-line chemotherapy for non-small

cell lung cancer, Cancer Treat Rev. 44 (2016) 42–50, https://doi.org/10.1016/j.ctrv.2016.01.003 Epub 2016/02/13. PubMed PMID: 26866673.
[19] G.S. Karagiannis, J.M. Pastoriza, Y. Wang, A.S. Harney, D. Entenberg, J. Pignatelli, et al., Neoadjuvant chemotherapy induces breast cancer metastasis through a TMEM-mediated mechanism, Sci. Transl. Med. 9 (397) (2017), https://doi.org/10.1126/scitranslmed.aan0026 Epub 2017/07/07. PubMed PMID: 28679654; PubMed Central PMCID: PMCPMC5592784.
[20] S. Ran, The role of TLR4 in chemotherapy-driven metastasis, Cancer Res. 75 (12) (2015) 2405–2410, https://doi.org/10.1158/0008-5472.can-14-3525 Epub 2015/05/23. PubMed PMID: 25998620; PubMed Central PMCID: PMCPMC4470764.
[21] I. Keklikoglou, C. Cianciaruso, E. Guc, M.L. Squadrito, L.M. Spring, S. Tazzyman, et al., Chemotherapy elicits pro-metastatic extracellular vesicles in breast cancer models, Nat. Cell Biol. 21 (2) (2019) 190–202, https://doi.org/10.1038/s41556-018-0256-3 Epub 2019/01/02. PubMed PMID: 30598531; PubMed Central PMCID: PMCPMC6525097.
[22] Y.S. Chang, S.P. Jalgaonkar, J.D. Middleton, T. Hai, Stress-inducible gene Atf3 in the noncancer host cells contributes to chemotherapy-exacerbated breast cancer metastasis, Proc. Natl. Acad. Sci. U. S. A 114 (34) (2017) E7159–E7168, https://doi.org/10.1073/pnas.1700455114 Epub 2017/08/09. PubMed PMID: 28784776; PubMed Central PMCID: PMCPMC5576783.
[23] J.H. Cho, J.Y. Jung, B.J. Lee, K. Lee, J.W. Park, Y. Bu, Epimedii herba: a promising herbal medicine for neuroplasticity, Phytother Res. : PTR 31 (6) (2017) 838–848, https://doi.org/10.1002/ptr.5807 Epub 2017/04/07. PubMed PMID: 28382688.
[24] I.R. Indran, R.L. Liang, T.E. Min, E.L. Yong, Preclinical studies and clinical evaluation of compounds from the genus Epimedium for osteoporosis and bone health, Pharmacol. Ther. 162 (2016) 188–205, https://doi.org/10.1016/j.pharmthera.2016.01.015 Epub 2016/01/29. PubMed PMID: 26820757.
[25] H. Ma, X. He, Y. Yang, M. Li, D. Hao, Z. Jia, The genus Epimedium: an ethnopharmacological and phytochemical review, J. Ethnopharmacol. 134 (3) (2011) 519–541, https://doi.org/10.1016/j.jep.2011.01.001 Epub 2011/01/11. PubMed PMID: 21215308.
[26] L.C. Ye, J.M. Chen, [Advances in study on pharmacological effects of Epimedium], Zhongguo Zhong yao za zhi = Zhongguo zhongyao zazhi = China journal of Chinese materia medica 26 (5) (2001) 293–295 Epub 2003/01/17. PubMed PMID: 12528515.
[27] R.A. Burim, D.I. Sendyk, L.S. Hernandes, D.F. de Souza, L. Correa, M.C. Deboni, Repair of critical calvarias defects with systemic epimedium sagittatum extract, J. Craniofac. Surg. 27 (3) (2016) 799–804, https://doi.org/10.1097/scs.0000000000002451 Epub 2016/03/17. PubMed PMID: 26982112.
[28] S. Di, C. Fan, Y. Yang, S. Jiang, M. Liang, G. Wu, et al., Activation of endoplasmic reticulum stress is involved in the activity of icariin against human lung adenocarcinoma cells, Apoptosis : Int. J. Program. Cell Death 20 (9) (2015) 1229–1241, https://doi.org/10.1007/s10495-015-1142-0 Epub 2015/06/08. PubMed PMID: 26049256.
[29] W. Li, M. Wang, L. Wang, S. Ji, J. Zhang, C. Zhang, Icariin synergizes with arsenic trioxide to suppress human hepatocellular carcinoma, Cell Biochem. Biophys. 68 (2) (2014) 427–436, https://doi.org/10.1007/s12013-013-9724-3 Epub 2013/08/27. PubMed PMID: 23975599.
[30] Z.F. Gu, Z.T. Zhang, J.Y. Wang, B.B. Xu, Icariin exerts inhibitory effects on the growth and metastasis of KYSE70 human esophageal carcinoma cells via PI3K/AKT and STAT3 pathways, Environ. Toxicol. Pharmacol. 54 (2017) 7–13, https://doi.org/10.1016/j.etap.2017.06.004 Epub 2017/07/02. PubMed PMID: 28667862.
[31] S. Li, P. Dong, J. Wang, J. Zhang, J. Gu, X. Wu, et al., Icariin, a natural flavonol glycoside, induces apoptosis in human hepatoma SMMC-7721 cells via a ROS/JNK-dependent mitochondrial pathway, Cancer Lett. 298 (2) (2010) 222–230, https://doi.org/10.1016/j.canlet.2010.07.009 Epub 2010/08/03. PubMed PMID: 20674153.
[32] Y. Guo, X. Zhang, J. Meng, Z.Y. Wang, An anticancer agent icaritin induces sustained activation of the extracellular signal-regulated kinase (ERK) pathway and inhibits growth of breast cancer cells, Eur. J. Pharmacol. 658 (2–3) (2011) 114–122, https://doi.org/10.1016/j.ejphar.2011.02.005 Epub 2011/03/08. PubMed PMID: 21376032; PubMed Central PMCID: PMCPMC3071461.
[33] R.L. Siegel, K.D. Miller, A. Jemal, Cancer statistics, 2018, CA A Cancer J. Clin. 68 (1) (2018) 7–30, https://doi.org/10.1016/j.ejphar.2011.02.005 Epub 2018/01/10. PubMed PMID: 29313949.
[34] M. Damelin, A. Bankovich, J. Bernstein, J. Lucas, L. Chen, S. Williams, et al., A PTK7-targeted antibody-drug conjugate reduces tumor-initiating cells and induces sustained tumor regressions, Sci. Transl. Med. 9 (372) (2017), https://doi.org/10.1126/scitranslmed.aag2611 Epub 2017/01/13. PubMed PMID: 28077676.
[35] L. Guilleminault, D. Carmier, N. Heuze-Vourc'h, P. Diot, E. Pichon, [Immunotherapy in non-small cell lung cancer: inhibition of PD1/PDL1 pathway], Rev. Pneumol. Clin. 71 (1) (2015) 44–56, https://doi.org/10.1016/j.pneumo.2014.11.004 Epub 2015/02/18. PubMed PMID: 25687821.
[36] J. Remon, B. Besse, J.C. Soria, Successes and failures: what did we learn from recent first-line treatment immunotherapy trials in non-small cell lung cancer? BMC Med. 15 (1) (2017) 55, https://doi.org/10.1186/s12916-017-0819-3 Epub 2017/03/14. PubMed PMID: 28285592; PubMed Central PMCID: PMCPMC5346853.
[37] Z. Yan, Z. Lai, J. Lin, Anticancer properties of traditional Chinese medicine, Comb. Chem. High Throughput Screen. 20 (5) (2017) 423–429, https://doi.org/10.2174/1386207320666170116141818 Epub 2017/01/18. PubMed PMID: 28093974.
[38] X. Deng, S. Chen, D. Zheng, Z. Shao, H. Liang, H. Hu, Icariin prevents H2O2-induced apoptosis via the PI3K/Akt pathway in rat nucleus pulposus intervertebral disc cells, Evid. Based Complement Altern. Med. : eCAM 2017 (2017) 2694261, https://doi.org/10.1155/2017/2694261 Epub 2017/05/26. PubMed PMID: 28536643; PubMed Central PMCID: PMCPMC5425849.
[39] J. Ding, Y. Tang, Z. Tang, X. Zu, L. Qi, X. Zhang, et al., Icariin improves the sexual function of male mice through the PI3K/AKT/eNOS/NO signalling pathway, Andrologia 50 (1) (2018), https://doi.org/10.1111/and.12802 Epub 2017/03/16. PubMed PMID: 28294371.
[40] P. Majtnerova, T. Rousar, An overview of apoptosis assays detecting DNA fragmentation, Mol. Biol. Rep. 45 (5) (2018) 1469–1478, https://doi.org/10.1007/s11033-018-4258-9 Epub 2018/07/20. PubMed PMID: 30022463.
[41] S. Elmore, Apoptosis: a review of programmed cell death, Toxicol. Pathol. 35 (4) (2007) 495–516, https://doi.org/10.1080/01926230701320337 Epub 2007/06/15. PubMed PMID: 17562483; PubMed Central PMCID: PMCPMC2117903.
[42] A. Fernandez, R. Ordonez, R.J. Reiter, J. Gonzalez-Gallego, J.L. Mauriz, Melatonin and endoplasmic reticulum stress: relation to autophagy and apoptosis, J. Pineal Res. 59 (3) (2015) 292–307, https://doi.org/10.1111/jpi.12264 Epub 2015/07/24. PubMed PMID: 26201382.
[43] A.X. Li, M. Sun, X. Li, Withaferin-A induces apoptosis in osteosarcoma U2OS cell line via generation of ROS and disruption of mitochondrial membrane potential, Eur. Rev. Med. Pharmacol. Sci. 21 (6) (2017) 1368–1374 Epub 2017/04/08. PubMed PMID: 28387888.
[44] Y.Y. Qiu, Y. Chen, T.H. Zeng, W.H. Guo, W.Y. Zhou, X.J. Yang, Hypoxia-induced apoptosis and mitochondrial dysfunction in chondrocytes arising from CREB phosphorylation reduction, Genet. Mol. Res. : GMR 15 (2) (2016), https://doi.org/10.4238/gmr.15027755 Epub 2016/06/21. PubMed PMID: 27323157.
[45] X.F. Song, H. Tian, P. Zhang, Z.X. Zhang, Expression of cyt-c-mediated mitochondrial apoptosis-related proteins in rat renal proximal tubules during development, Nephron 135 (1) (2017) 77–86, https://doi.org/10.1159/000450585 Epub 2016/09/26. PubMed PMID: 27665619.
[46] D.J. Granville, B.A. Cassidy, D.O. Ruehlmann, J.C. Choy, C. Brenner, G. Kroemer, et al., Mitochondrial release of apoptosis-inducing factor and cytochrome c during smooth muscle cell apoptosis, Am. J. Pathol. 159 (1) (2001) 305–311, https://doi.org/10.1016/s0002-9440(10)61696-3 Epub 2001/07/05. PubMed PMID: 11438477; PubMed Central PMCID: PMCPMC1850399.
[47] A. Yao, Y. Shen, A. Wang, S. Chen, H. Zhang, F. Chen, et al., Sulforaphane induces apoptosis in adipocytes via Akt/p70s6k1/Bad inhibition and ERK activation, Biochem. Biophys. Res. Commun. 465 (4) (2015) 696–701, https://doi.org/10.1016/j.bbrc.2015.08.049 Epub 2015/08/25. PubMed PMID: 26296464.
[48] H. Zhou, Q. Hou, Y. Chai, Y.T. Hsu, Distinct domains of Bcl-XL are involved in Bax and Bad antagonism and in apoptosis inhibition, Exp. Cell Res. 309 (2) (2005) 316–328, https://doi.org/10.1016/j.yexcr.2005.06.014 Epub 2005/08/03.. PubMed PMID: 16061221.
[49] E. Yang, J. Zha, J. Jockel, L.H. Boise, C.B. Thompson, S.J. Korsmeyer, Bad, a heterodimeric partner for Bcl-XL and Bcl-2, displaces Bax and promotes cell death, Cell 80 (2) (1995) 285–291 Epub 1995/01/27. PubMed PMID: 7834748.
[50] H. Li, J. Hu, S. Wu, L. Wang, X. Cao, X. Zhang, et al., Auranofin-mediated inhibition of PI3K/AKT/mTOR axis and anticancer activity in non-small cell lung cancer cells, Oncotarget 7 (3) (2016) 3548–3558, https://doi.org/10.18632/oncotarget.6516 Epub 2015/12/15. PubMed PMID: 26657290; PubMed Central PMCID: PMCPMC4823126.
[51] C. Perez-Ramirez, M. Canadas-Garre, M.A. Molina, M.J. Faus-Dader, M.A. Calleja-Hernandez, PTEN and PI3K/AKT in non-small-cell lung cancer, Pharmacogenomics 16 (16) (2015) 1843–1862, https://doi.org/10.2217/pgs.15.122 Epub 2015/11/12. PubMed PMID: 26555006.
[52] W.F. Chen, L. Wu, Z.R. Du, L. Chen, A.L. Xu, X.H. Chen, et al., Neuroprotective properties of icariin in MPTP-induced mouse model of Parkinson's disease: involvement of PI3K/Akt and MEK/ERK signaling pathways, Phytomedicine : Int. J. Phytother. Phytopharmacol. 25 (2017) 93–99, https://doi.org/10.1016/j.phymed.2016.12.017 Epub 2017/02/14. PubMed PMID: 28190476.
[53] H. Zhang, Z. Xiong, J. Wang, S. Zhang, L. Lei, L. Yang, et al., Glucagon-like peptide-1 protects cardiomyocytes from advanced oxidation protein product-induced apoptosis via the PI3K/Akt/Bad signaling pathway, Mol. Med. Rep. 13 (2) (2016) 1593–1601, https://doi.org/10.3892/mmr.2015.4724 Epub 2016/01/01. PubMed PMID: 26717963; PubMed Central PMCID: PMCPMC4732836.
[54] Z. Fu, J. Yang, Y. Wei, J. Li, Effects of piceatannol and pterostilbene against beta-amyloid-induced apoptosis on the PI3K/Akt/Bad signaling pathway in PC12 cells, Food Funct. 7 (2) (2016) 1014–1023, https://doi.org/10.1039/c5fo01124h Epub 2016/01/14. PubMed PMID: 26757883.